Journal Homepage: http://ijcpe.uobaghdad.edu.iq
Iraqi Journal of Chemical and Petroleum Engineering
Vol. 26 No. 1 (March 2025) 89 – 97
EISSN: 2618-0707, PISSN: 1997-4884

Adsorptive desulfurization of benzothiophene from simulated fuel using Ni/ Γ-Al_2O_3 as an adsorbent; performance, adsorption, and kinetic study

Nawar Yaqoob [a, *], Tariq M. Naife [a], Zaid Nidhal Shareef [b]

a Department of Chemical Engineering, College of Engineering, University of Baghdad, Baghdad, Iraq
b Curtin University, Chemical Engineering Department, Australia

Abstract

Adsorptive desulfurization is essential for supplying clean fuel, reducing environmental pollution, and obtaining strict regulatory standards. This study focused on the adsorptive desulfurization of benzothiophene from simulated fuel using Ni/ γ-Al_2O_3 as an adsorbent. The study investigated the effect of nickel ions loading percentage on the removal efficiency. Also, the most fitted kinetic and isotherm models for the process were indicated. The modified adsorbent was characterized by different techniques, including XRD, FESEM, and EDS. The measurements revealed a successful modification of Ni/ γ-Al_2O_3, achieving the required loading percentages (2-10%). The desulfurization investigation was carried out under varying conditions of adsorbent dose (0.2-1 g), Ni loading percentage (2-10%), initial sulfur level of 100-260 ppm, and contact time (15-600 min). The results showed that Ultra-deep desulfurization was accomplished, with 96% sulfur removed from the initial concentration of 100 ppm at 1 g of adsorbent under room temperature and atmospheric pressure, 10% Ni ions content, and 600 min of contact time, and the highest adsorption capacity was 57.2 mg S/ g adsorbent at 260 ppm. The Langmuir isotherm model best described the process with R^2 of 99.9%, while the pseudo-second-order kinetic model had R^2 of 99.99%.

Keywords: Gamma alumina oxide; ion exchange; Adsorptive Desulfurization; Adsorption isotherms models; kinetic models.

Received on 05/04/2024, Received in Revised Form on 30/07/2024, Accepted on 30/07/2024, Published on 30/03/2025

https://doi.org/10.31699/IJCPE.2025.1.9

1- Introduction

Crude oil is the world's most widely used and reasonably priced energy source. The primary byproducts of crude oil utilized in cars are gasoline, kerosene, and diesel, fuels mostly contain sulfur compounds in the form of organic sulfur compounds (OSCs) [1].

Examples of aromatic sulfur-containing compounds are benzothiophene (BT), dibenzothiophene (DBT), and 4,6dimethyl benzothiophene. It is well known that these substances have the potential to cause cancer. Furthermore, the products of these reactions also have a significant role in raising the fuel's total sulfur content [2].

BT stands for benzothiophene, an aromatic sulfur compound with the chemical formula C8H6S, a molecular size of 6 Å, a boiling point of (220–221) °C, and a smell comparable to naphthalene. One of the most refractory sulfur compounds, it is present in the light diesel, jet fuel (kerosene), and heavy gasoline ranges. Its reactive sites enable functionalization even though the molecule is generally stable [3].

Sulfur compounds are thought to be the primary source of atmospheric sulfur emissions, a serious environmental hazard. When sulfur and its derivatives in transportation fuels burn, they quickly turn into SO2 and fine particles, which are airborne main pollutants that harm the environment and public health by causing smog, acid rain, and dry deposition [4]. Additionally, any sulfur present in fuels could provide a risk of poisoning the catalyst utilized in the refining process, the equipment in refineries may have corrosion issues as a result of catalysts deactivating more quickly [5].

Many countries throughout the world have enacted environmental legislation aimed at reducing the sulfur content of fuel fractions to incredibly low levels (10 parts per million). As a result, air quality has improved, and transportation fuel machines' harmful emissions have decreased [6].

Consequently, fuel desulfurization can be an extremely important technique for the oil sector, and new approaches that are highly cost-effective and efficient while also satisfying environmental regulations and purifying standards must be found. Hydrodesulfurization (HDS), extractive distillation, selective adsorption, bio-desulfurization, and oxidative desulfurization (ODS) are only a few of the techniques used to remove sulfur compounds from fuel oil [7].

The HDS method is used by refineries all over the world, however it has a lot of disadvantages. Hydrodesulfurization (HDS) processes are often run at high pressures (5–13 MPa) and temperatures between 300

*Corresponding Author: Email: Nawar.yaqoob1607m@coeng.uobaghdad.edu.iq

and 400 °C. High hydrogen consumption increases running expenses. Operating challenges are increased by catalyst fouling and pressure loss. One major man-made air pollution source is hydrogen sulfide gas released by hydrotreaters [8, 9].

Adsorption is a selective method that removes sulfur from fuels. Its primary goal is to do so while leaving non-sulfur containing hydrocarbons including aromatic, olefin, and cyclic paraffinic hydrocarbons unaltered [10].

Adsorption-based desulfurization offers several benefits over other methods since it may directly adsorb refractory chemicals utilizing a variety of solid adsorbent materials at ambient temperature and atmospheric pressure in straightforward operating conditions. Due to its low energy consumption and lack of expensive high-pressure hydrogen reactors or corrosive oxidants, it is a cost-effective process. This also simplifies the design of the adsorber significantly compared to other desulfurization methods previously addressed [11].

In this research, Ni ions were successfully loaded on the support γ-Al_2O_3through batch wet impregnation and characterized by FESEM, XRD, and EDS. Then, it was used to investigate its performance in the desulfurization of benzothiophene from simulated fuel and the role of active metal sites in enhancing the adsorption removal through chemisorption. In addition, the most fitted adsorption isotherms and kinetic models for the process were found.

2- Experimental work

2.1. Materials

All materials used for the modification part and the removal process are given below in Table 1.

Table 1. The materials that were used for the study work

Material	Chemical Formula	Supplied Company	Origin	Phase
Gamma Alumina	γ-Al_2O_3	Hunano material	China	Powder
Aqueous Nickel Nitrate	$Ni(NO_3)_2.6H_2O$	CDH fine chemicals	India	Solid crystals
Distilled Water	H_2O	University Lab	Lab	Liquid
Normal Hexane	$CH_3(CH_2)_4.CH_3$	CDH fine chemicals	India	Liquid
Benzothiophene	C_8H_6S	Sigma-Aldrich	USA	Solid crystals

2.2. Adsorbent modification

The modification of the procedure of γ-Al_2O_3 was adjusted accordingly to (A. H. M. S. Hussain) [12] :

A 500 ml three-neck drum flask was attached to reflux and used for the modification process. 100 ml of distilled water was mixed with (0.4-2 g) of $Ni(NO_3)_2.6H_2O$ for 30 min under 80 °C and 250 rpm for dissolving different concentrations of $Ni(NO_3)_2.6H_2O$ to produce the needed percentage of Ni ions. 4 g of γ-Al_2O_3 was added and mixed at 300 rpm and 600 rpm respectively overnight at 80 °C. The solution was separated by evaporation in the oven at 60 °C for overnight. The solid material was calcined at 420 °C for 5h with a temperature rate of 2.33 °C/ min for evaporating of NO_3 and other impurities.

2.3. Batch adsorption

Four different simulated fuels were prepared by adding 0.419, 0.838, and 1.08 g of Benzothiophene to 100 ml of N-Hexane each time to produce model fuels containing varying initial sulfur concentrations with ranges of 100, 200, and 260 ppm.

The 250 ml conical flask was used for the batch adsorption studies (1990 Germany). 100 ml of the simulated fuel was poured in the flask and a predetermined amount of the adsorbent was introduced. The conical flask was closed and left in the shaker for a specific time at room temperature and atmospheric pressure and 200 rpm. In order to optimize surface area for mass transfer, reduce agitation for suspension, and reduce resistance to mass transfer, the adsorbents utilized in this procedure were powdered.

Throughout the investigation, the effects of initial sulfur concentration (100–260 mg/L), adsorbent dosage (0.2–1 g), Ni ions loading percentage (2-10 %), and contact time (15–600 min) on adsorption capacity and removal efficiency were examined.

All adsorbents were in powder form for mass transfer optimization and reducing the agitation. After each run, a small sample of the fuel was withdrawn and sent for a total sulfur content analyzer.

Removal of sulfur content was shown as Desulfurization efficiency (DS%) which is calculated as the ratio of sulfur removed to that initially present in fuel [13].

$$DS\ \% = \frac{C_o - C}{C_o} * 100 \quad (1)$$

Where: C_o: the initial sulfur content in fuel. C: the measured sulfur content in fuel.

To determine the adsorption capacity, the following equations were used:

$$qe = \frac{Co - Ce}{m} x\ V \quad (2)$$

$$qt = \frac{Co - Ct}{m} x\ V \quad (3)$$

Where: q_e: adsorption capacity at equilibrium mg/g. q_t: adsorption capacity at sampling time mg/g. V: volume of model fuel in L. M: mass of adsorbent in g. C_o, C_e, and C_t are sulfur content at initial, equilibrium, and intervals sampling time respectively in ppm.

3- Results and discussion

3.1. Characterization of adsorbent

X-ray diffraction XRD was the most crucial analysis used to determine whether Ni exists and to understand its crystalline characteristics. The XRD patterns of

adsorbents are illustrated in Fig. 1. The XRD pattern shows recognizable diffraction peaks. The peaks of aluminum oxide at 2θ= 32.15°, 37.55°, 45.77°, and 66.92° are the characteristics peaks of the γ-Al_2O_3 phase. The peak at 2θ of 44.8° corresponds to metallic Ni (111) lattice planes. This result is in agreement with [14, 15].

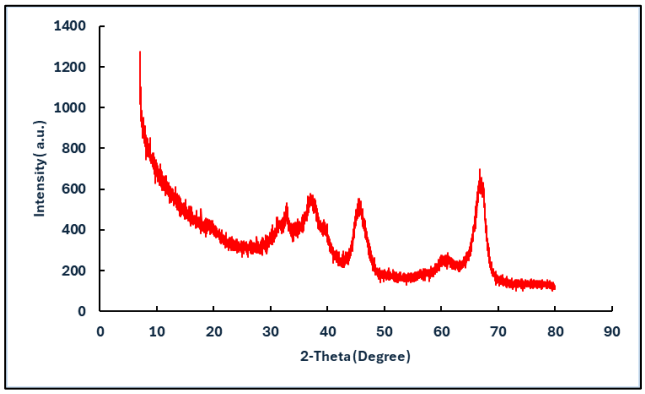

Fig. 1. XRD pattern of modified Ni/ γ-Al_2O_3

The morphology of the surface of the Ni/ γ-Al_2O_3 sample is acquired at a magnification of 60 kx and zoom of 1 um. The FESEM images of Ni/ γ-Al_2O_3 adsorbent powder shown in Fig. 2 indicated the porous structure of γ-Al_2O_3 and the nano size particles. The particles seem to suffer from agglomeration and have a relatively hexagonal shape. This result is in line with the earlier research [16].

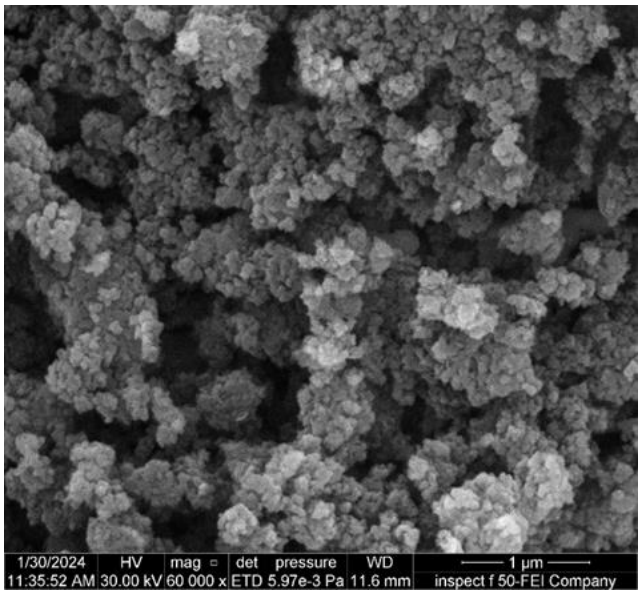

Fig. 2. FESEM of modified Ni/ γ-Al_2O_3

EDS characterization technique was employed for the elemental analysis of modified Ni/ γ-Al_2O_3. The techniques examined the X-rays that a substance emits when it is exposed to electromagnetic radiation. Also, the weight percentage of each element was counted as shown in Table 2. It was revealed that the elements percentages of Ni/ γ-Al_2O_3 are 44.5% of Al, 54.7% of O, and 1.8% of Ni. This result approved the high purity of supplied γ-Al_2O_3 and the successful Ni loading process through wet impregnation for the required percentage.

Table 2. EDS result of Ni/γ-Al_2O_3

Samples	Element	Weight%	Weight % Error
	O	54.7	0.3
1	Al	44.5	0.2
	Ni	1.8	0.1
	O	53.5	0.1
2	Al	42.6	0.2
	Ni	3.9	0.3
	O	52.3	0.2
3	Al	41.6	0.4
	Ni	6.1	0.1
	O	51.2	0.2
4	Al	40.6	0.3
	Ni	8.2	0.3
	O	50.4	0.4
5	Al	39.8	0.1
	Ni	9.8	0.2

3.2. Effect of nickel loading

As shown in Fig. 3 the effect of nickel loading percentage was studied using model fuel of 100 ml n-hexane and 100 ppm of benzothiophene under 200 rpm shaking, 0.6 g of Ni/ γ-Al_2O_3 and for 120 min of contact time. It is obvious that the desulfurization process was not successful at 0% of Ni which indicates that γ-Al_2O_3 is not efficient for the removal of sulfur. This can be due to the high pore size of the used γ-Al_2O_3 (18.42 nm). Also, γ-Al_2O_3 has no metal active sites which is responsible for reactive desulfurization through interacting with sulfur in order to form sigma bonds. Fig. 3 indicates that the removal efficiency increased from 44% at 2% of Ni loading to 73% at 10% of Ni loading, which shows that the removal efficiency enhanced as the metal loading percentage increased. This result agrees with earlier research [17] which found Ni has strong molecular orbitals that can attract hindered benzothiophene and other cyclic sulfur compounds, donating electron density to the metal and forming an effective connection with it.

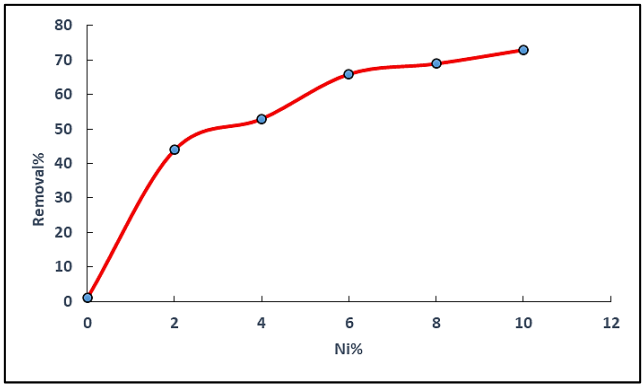

Fig. 3. Effect of nickel loading percentage on removal efficiency

3.3. Effect of adsorbent dose

Fig. 4 illustrates the effect of the adsorbent dose on the adsorptive desulfurization efficiency. The adsorbent dose

varied from 0.2 g to 1 g of Ni/ γ-Al_2O_3 adsorbent. The effect of the adsorbent dose was investigated under conditions of atmospheric pressure and room temperature, 100 ml of simulated fuel containing 100 ppm of sulfur, 10% of Ni ions loading, 120 min of contact time, and 200 rpm of shaking. As illustrated by Fig. 4 the removal efficiency of benzothiophene increased from 32% for 0.2 g to 96% for 1 g of adsorbent. This phenomenon can be explained that as the adsorbent dose increases the available surface metal active sites for desulfurization will be increased in which boosts the driving force for the removal [18].

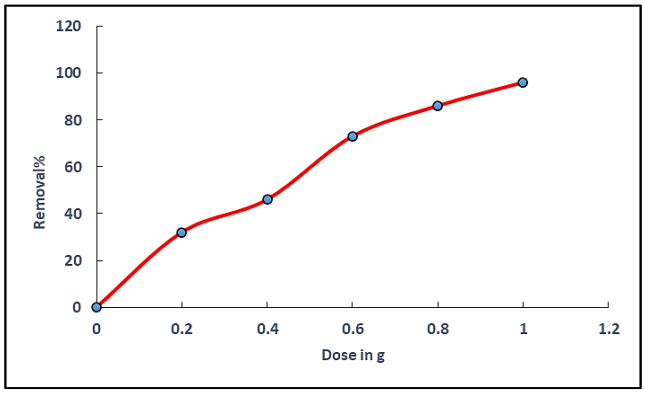

Fig. 4. Effect of adsorbent dose on removal efficiency

3.4. Effect of sulfur initial concentration

Fig. 5 shows the impact of the initial sulfur ion concentration on the desulfurization efficiency within the range of (100-260) ppm under the following conditions: 120 min of contact time, 200 rpm shaking speed, 1g of Ni/ γ-Al_2O_3 adsorbent with 10% of Ni loaded, and 100 ml of simulated fuel. Ultra-deep desulfurization was achieved for 100 ppm where desulfurization efficiency reached 96% of removal while it started to decrease further for initial concentrations beyond 100 ppm declining to 88% removal at 260 ppm. The maximum capacity achieved at 260 ppm was 57.2 mg/g. This decline in removal may be results from increasing sulfur concentrations in the simulated fuel while the active sites remain constant. So, the sulfur was in excess, and adsorption beyond equilibrium couldn't be applied [19].

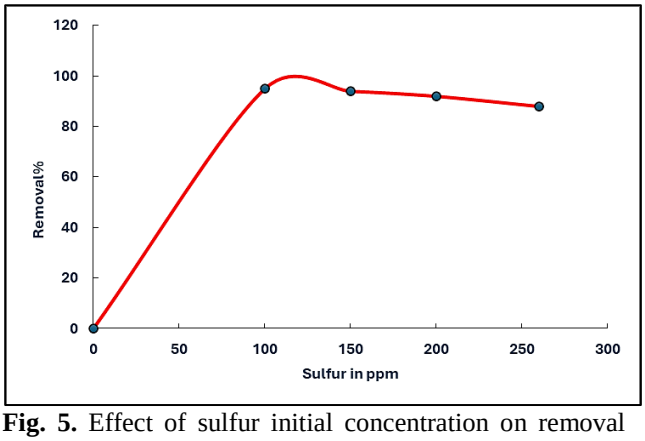

Fig. 5. Effect of sulfur initial concentration on removal efficiency

3.5. Effect of contact time

As shown by Fig. 6 the contact time was varied from 15 min to 600 min to study the effect of contact time under the conditions of 100 ml of simulated fuel containing 100 ppm of sulfur, 200 rpm of shaking speed, 1g of Ni/ γ-Al_2O_3 adsorbent, atmospheric pressure and room temperature. Most of the removal occurred within the first 15 minutes of the process. After that, the adsorption capacity of adsorption increases until it reaches equilibrium at 60 min of contact with BT. Furthermore, no more reasonable desulfurization appeared. According to [20] the adsorbent active sites are engaged gradually with the sulfur compound for a certain contact time until the saturation capacity is reached, and the highest adsorption occurred. Furthermore, no significant desulfurization occurred no matter how much contact time increased.

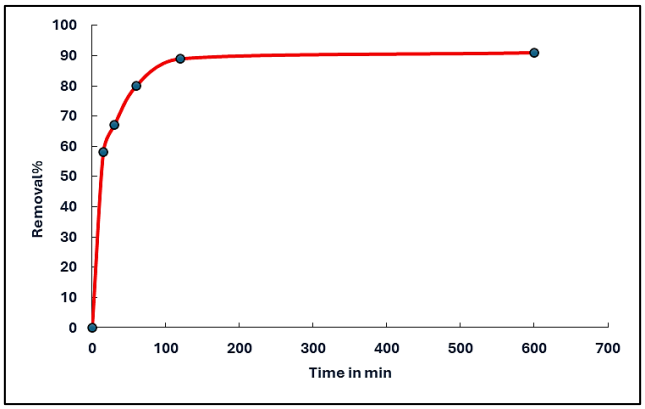

Fig. 6. Effect of contact time on removal efficiency

3.6. Adsorption isotherm models

Adsorption isotherms offer a precise explanation of the relationship that exists between the amount of adsorbent (qe) and the amount of adsorbate that is still present (Ce) in an equilibrium state at a constant temperature [4]. Adsorption isotherms allow one to quantify the adsorbate concentration in the case of a liquid and the pressure in the case of a gas, as well as fully comprehend the relationship between the dissolved compounds and the adsorbent in the solution. One can also use adsorption isotherms to determine the ideal adsorption conditions by examining the nature of adsorption [21]. Adsorption isotherms also show how molecules are dispersed in the medium of the liquid and solid phases once the process has reached an equilibrium state. The link between the amount of adsorbate and the adsorbent's surface temperature is used to categorize the adsorption phenomena. However, a new equilibrium also causes a corresponding shift in concentration [21].

3.6.1. Langmuir model

The Langmuir model can determine whether or not a monolayer is adsorbed; otherwise, there is no contact between the adsorbed molecules. The Langmuir equation

is valid for a single monolayer adsorbed with a well-defined number of energetically identical and homogeneous adsorption sites [2]. Eq.4 and Eq.5 describe the Langmuir adsorption isotherm for the linear case [13].

$$q_e = \frac{q_{max} K_L C_e}{1 + K_L C_e} \quad (4)$$

$$\frac{1}{q_e} = \frac{1}{q_{max} K_L} \frac{1}{C_e} + \frac{1}{q_{max}} \quad (5)$$

Where: q_e: adsorption capacity when equilibrium is achieved described by units of mg/g. C_e: the adsorbed concentration at equilibrium by units of mg/l. q_{max}: adsorption capacity at maximum by units of mg/g. K_L: Langmuir constantly expressed the binding sites in units of l/mg.

3.6.2. Freundlich model

The Freundlich model assumes that the adsorption process happens in a multilayer suspension in which the molecular distribution is heterogeneous on the surface of the adsorbent [22]. Eq. 6 is a mathematical illustration of the isotherm. Whereas Eq. 7 is the linear form of the isotherm model of Freundlich [23]

$$q_e = K_F \, C_e^{\frac{1}{n}} \quad (6)$$

$$ln \, q_e = ln \, K_F + \frac{1}{n} ln \, C_e \quad (7)$$

Where: q_e: represents adsorption capacity when equilibrium is reached (mg/g). K_F: is known as the Freundlich constant which represents the calculated capacity of adsorption $[(mg.g^{-1}).(mg^{-1})^{1/n}]$. n: is the intensity value for adsorption which determines adsorption type.

3.6.3. Temkin model

Temkin's model characterizes adsorption as a uniform distribution of binding energy up to its maximum value. The number of metal ions adsorbed was found to be directly proportional to the number of active sites on the adsorbent material's surface. Using Temkin's model, we can determine the adsorption energy and interactions between ions and the adsorbent [13]. To apply the Temkin isotherm, use Eq.8. [24]

$$q_e = B \, ln \, K_T + B \, ln \, C_e \quad (8)$$

Where B and K_T are the Temkin energy constant (J/mol) and the constant describing the interaction between sulfur molecules and adsorbent surface (dimensionless), respectively.

The application of Eqs. 5, 7, and 8 results in Fig. 7, Fig. 8, Fig. 9, and Table 3, which display the parameters and correlation coefficients for each adsorption isotherm. Table 3 makes it evident that the Langmuir isotherm was the most appropriate for sulfur removal since R^2 (99.9%) is the closest to unity. For the specified concentration range, the Langmuir isotherm characterizes the presence of the adsorbate monolayer (S) at the adsorbent surface. The Langmuir adsorption isotherm, according to [13], is an empirical equation that presupposes monolayer homogenous adsorption on the adsorbent surface. According to the Freundlich adsorption isotherm equation, n has a value of 2.1.

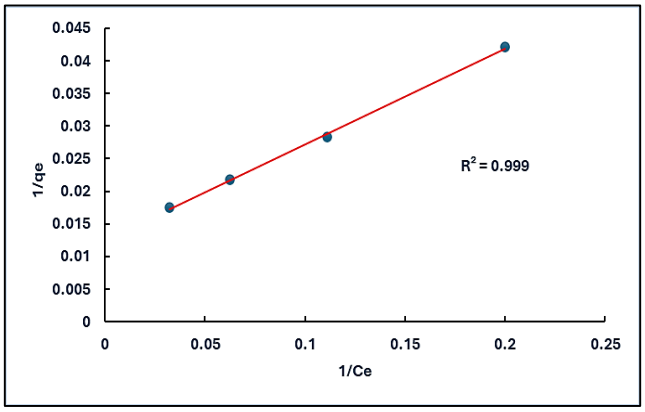

Fig. 7. Langmuir adsorption isotherm plot

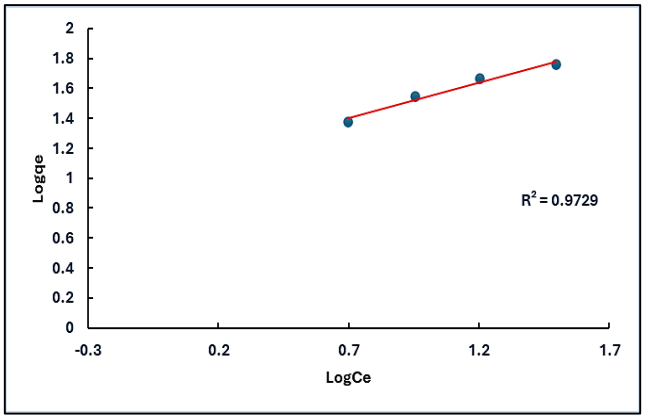

Fig. 8. Freundlich adsorption isotherm plot

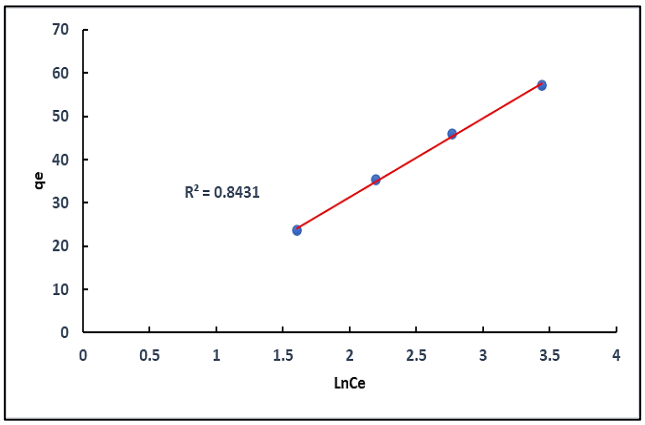

Fig. 9. Temkin adsorption isotherm plot

Table 3. The constants of the adsorption isotherms model

Langmuir model			Freundlich model			Temkin model		
K_L	q_m	R^2	K_F	n	R^2	BT	K_T	R^2
0.085	80	99.9%	11.68	2.1	97.2	102.51	9.25	84.3

3.7. Adsorption kinetic models

Adsorption kinetics is the study of the amount of adsorbent adsorbed over time. The speed of the adsorption process can be determined by studying its kinetics. It is beneficial to research the mechanism of the entire adsorption process and evaluate adsorbent quality [25].

3.7.1. Pseudo-1st order model

It assumed that adsorption occurred in a single layer on the adsorption surface between the liquid and solid phases. Additionally, pseudo-1st order was used to describe the early stages of adsorption phenomena. This model is described by the following linear equation: [13]

$$\ln(q_e - q_t) = \ln q_e - k_1 t \quad (9)$$

Where: q_t is the adsorbate quantity which adsorbent take in specific time (mg/g), q_e is adsorption capacity at equilibrium (mg/g) and k_1 is the Constant rate (1/min).

3.6.2. pseudo-second-order model

This kinetic model predicts behavior over the whole adsorption range, assuming that chemical sorption, or chemisorption, is the rate-limiting step. Under these conditions, the adsorption rate depends more on the adsorption capacity than the adsorbate concentration, hence the linearized Eq. 10 is written as follows [26].

$$\frac{t}{q_t} = \frac{1}{k_2 q_e^2} + \frac{1}{q_e} t \quad (10)$$

Where: q_t: the amount of adsorbate which adsorbent adsorbed in a specific time (mg/g). q_e: Capacity of adsorption at equilibrium (mg/g). K_2: Constant rate (1/min).

Both of the used models, pseudo-first order and pseudo-second order have been used to calculate the kinetic data for the adsorption of Sulfur on Ni/ γ-Al_2O_3 as an adsorbent. The two applied models' correlation factors and other parameters are listed in Table 4. As can be seen from Fig. 10 and Fig. 11, the pseudo-second order model, which has the highest correlation factor for applied models, is very close to unity (99.9%), making it the best model to represent and describe the experimental data. Pseudo Second Order is a good model to describe the adsorptive desulfurization of sulfur by Ni/ γ-Al_2O_3.

Table 4. The parameters of pseudo-first order model and pseudo-second order model

Pseudo-first order model			Pseudo-second order model		
q_e	K_1	R^2	q_e	K_2	R^2
13.94	-0.0000035	0.4299	69.93	0.0025	99.9

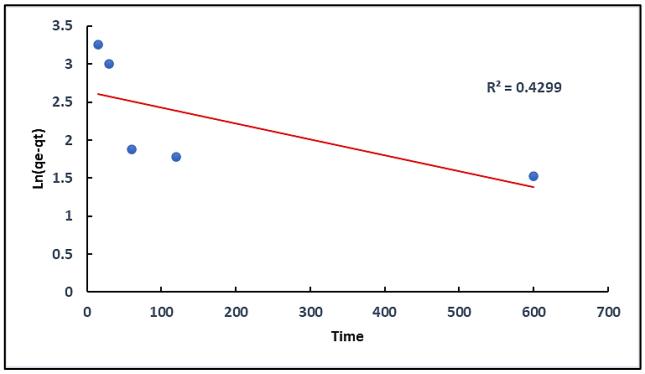

Fig. 10. The pseudo-first order kinetic model plot

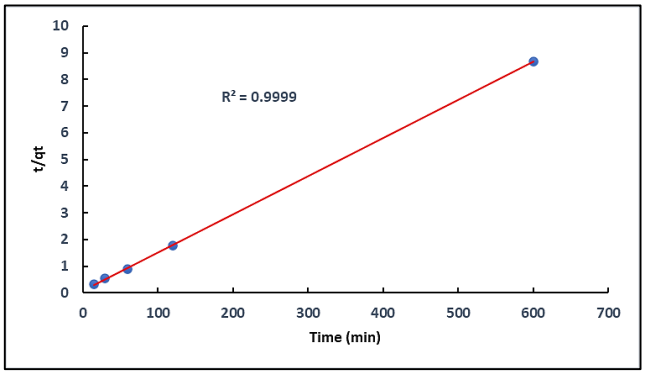

Fig. 11. The pseudo-second order kinetic model plot

4- Conclusion

Modifying γ-Al_2O_3 to produce Ni/ γ-Al_2O_3 was successfully conducted with varying content of Ni (2-10%). The loading process was successfully indicated through different techniques, including XRD, FESEM, and EDS, which approved the presence of the required percentage of Ni ions on the gamma alumina oxide. Ultra-deep desulfurization for simulated fuel was successfully achieved (96%) for simulated fuel with 100 ppm sulfur content by the modified adsorbent, which approved the role of metal active sites for desulfurization enhancement. It was found that the best conditions for the removal were 10% of Ni ions loading, 1 g of adsorbent dose, and 120 min of contact time. The research results of BT desulfurization by Ni/ γ-Al_2O_3 were fully explained by the Langmuir isotherm model and the pseudo-second-order model proving the monolayer chemisorption.

References

[1] Q. A. Mahmood, B. A. Abdulmajeed, and R. Haldhar, "Oxidative Desulfurization of Simulated Diesel Fuel by Synthesized Tin Oxide Nano-Catalysts Support on Reduced Graphene Oxide," *Iraqi Journal of Chemical and Petroleum Engineering*, vol. 24, no. 4, pp. 83–90, 2023, https://doi.org/10.31699/IJCPE.2023.4.8

[2] G. K. Jabaar, H. A. Al-jendeel, and Y. Ali, "Desulphurization of Simulated Oil Using SAPO-11 with CNT ' s as Adsorbent : A Kinetic Study," *Iraqi Journal of Chemical and Petroleum Engineering*, vol. 24, no. 3, pp. 69–77, 2023, https://doi.org/10.31699/IJCPE.2023.3.7

[3] R. Contreras *et al.*, "Transformation of thiophene, benzothiophene and dibenzothiophene over Pt/HMFI, Pt/HMOR and Pt/HFAU: Effect of reactant molecular dimensions and zeolite pore diameter over catalyst activity," *Catalysis Today*, vol. 130, no. 2–4, pp. 320–326, 2008, https://doi.org/10.1016/j.cattod.2007.10.007

[4] B. D. Radhi and W. T. Mohammed, "Novel nanocomposite adsorbent for desulfurization of 4,6-dimethyldibenzothiophene from model fuel," *Materials Today Proceedings*, vol. 42, pp. 2880–2886, 2021, https://doi.org/10.1016/j.matpr.2020.12.738

[5] M. A. Betiha, A. M. Rabie, H. S. Ahmed, A. A. Abdelrahman, and M. F. El-Shahat, "Oxidative desulfurization using graphene and its composites for fuel containing thiophene and its derivatives: An update review," *Egyptian Journal of Petroleum*, vol. 27, no. 4, pp. 715–730, 2018, https://doi.org/10.1016/j.ejpe.2017.10.006

[6] M. M. Yahya and H. Q. Hussein, "Adsorption Desulfurization Of Iraqi Heavy Naphtha Using Zeolite 13x," *Association of Arab Universities Journal of Engineering Sciences*, vol. 26, no. 2, pp. 12–18, 2019, https://doi.org/10.33261/jaaru.2019.26.2.003

[7] B. A. Altabbakh, M. N. Abbas, H. M. Hussain, and S. K. Hussain, "Preparation of Supported Bimetallic Ce/Fe activated carbon for Desulfurization reaction," *Journal of Petroleum Research and Studies*, vol. 12, no. 1, pp. 173–190, 2022, https://doi.org/10.52716/jprs.v12i1.597

[8] F. J. Méndez, O. E. Franco-López, X. Bokhimi, D. A. Solís-Casados, L. Escobar-Alarcón, and T. E. Klimova, "Dibenzothiophene hydrodesulfurization with NiMo and CoMo catalysts supported on niobium-modified MCM-41," *Applied Catalysis B: Environmental*, vol. 219, pp. 479–491, 2017, https://doi.org/10.1016/j.apcatb.2017.07.079

[9] K. O. Blumberg, M. P. Walsh, and C. Pera, "Low-Sulfur Gasoline and Diesel: The Key to Lower Vehicle Emissions," *The international council on clean transportation*, May, p. 66, 2003.

[10] H. J. Mousa and H. Q. Hussein, "Adsorptive Desulfurization of Iraqi Heavy Naphtha Using Different Metals over Nano Y Zeolite on Carbon Nanotube," *Iraqi Journal of Chemical and Petroleum Engineering*, vol. 21, no. 1, pp. 23–31, 2020, https://doi.org/10.31699/IJCPE.2020.1.4

[11] B. Radhi and W. Mohammed, "TiO2 loading on activated carbon: preparation, characterization, desulfurization performance and isotherm of the adsorption of dibenzothiophene from model fuel," *Egyptian Journal of Chemistry*, vol. 66, no7. 0, pp. 428 - 437, 2023, https://doi.org/10.21608/ejchem.2022.109702.5003

[12] A. H. M. S. Hussain and B. J. Tatarchuk, "Adsorptive desulfurization of jet and diesel fuels using Ag/TiO x-Al2O3 and Ag/TiOx-SiO2 adsorbents," *Fuel*, vol. 107, pp. 465–473, 2013, https://doi.org/10.1016/j.fuel.2012.11.030

[13] N. Jawad and T. M. Naife, "Mathematical Modeling and Kinetics of Removing Metal Ions from Industrial Wastewater," *Iraqi Journal of Chemical and Petroleum Engineering*, vol. 23, no. 4, pp. 59–69, 2022, https://doi.org/10.31699/IJCPE.2022.4.8

[14] L. He, Y. Ren, B. Yue, S. C. E. Tsang, and H. He, "Tuning metal–support interactions on ni/al2 o3 catalysts to improve catalytic activity and stability for dry reforming of methane," *Processes*, vol. 9, no. 4, 2021, https://doi.org/10.3390/pr9040706

[15] F. Kanwal, A. Batool, M. Adnan, and S. Naseem, "The effect of molecular structure, band gap energy and morphology on the dc electrical conductivity of polyaniline/aluminium oxide composites," *Materials Research Innovations*, vol. 19, April 2018, pp. 354–358, 2015, https://doi.org/10.1179/1432891715Z.0000000001688

[16] A. H. A. K. Mohammed, H. Q. Hussein, and M. S. Mohammed, "The Effect of Crystallization Time and Acid Type on the Synthesis of Nano-Gamma Alumina Using Double Hydrothermal Method," *Iraqi Journal of Chemical and Petroleum Engineering*, vol. 18, no. 2, pp. 1–11, 2017, https://doi.org/10.31699/IJCPE.2017.2.1

[17] K. K. Sarda, A. Bhandari, K. K. Pant, and S. Jain, "Deep desulfurization of diesel fuel by selective adsorption over Ni/Al 2O 3 and Ni/ZSM-5 extrudates," *Fuel*, vol. 93, pp. 86–91, 2012, https://doi.org/10.1016/j.fuel.2011.10.020

[18] T. A. Saleh, K. O. Sulaiman, S. A. AL-Hammadi, H. Dafalla, and G. I. Danmaliki, "Adsorptive desulfurization of thiophene, benzothiophene and dibenzothiophene over activated carbon manganese oxide nanocomposite: with column system evaluation," *Journal of Cleaner Production*, vol. 154, pp. 401–412, 2017, https://doi.org/10.1016/j.jclepro.2017.03.169

[19] S. K. Thaligari, V. C. Srivastava, and B. Prasad, "Adsorptive desulfurization by zinc-impregnated activated carbon: characterization, kinetics, isotherms, and thermodynamic modeling," *Clean Technologies and Environmental Policy*, vol. 18, no. 4, pp. 1021–1030, 2016, https://doi.org/10.1007/s10098-015-1090-y

[20] X.F.Zhang, Z. Wang , Y. Feng , Y.Zhong , J. Liao, Y. Wang , J. Yao., "Adsorptive desulfurization from the model fuels by functionalized UiO-66(Zr)," *Fuel*, vol. 234, no. July, pp. 256–262, 2018, https://doi.org/10.1016/j.fuel.2018.07.035

[21] N. Gaur, K. Narasimhulu, and Y. PydiSetty, "Recent advances in the bio-remediation of persistent organic pollutants and its effect on environment," *Journal of Cleaner Production*, vol. 198, pp. 1602–1631, 2018, https://doi.org/10.1016/j.jclepro.2018.07.076

[22] Z. N. Jamka and W. T. Mohammed, "Assessment of the Feasibility of Modified Chitosan Beads for the Adsorption of Nitrate from an Aqueous Solution," *Journal of Ecological Engineering*, vol. 24, no. 2, pp. 265–278, 2023, http://dx.doi.org/10.12911/22998993/156886

[23] S. M. Al-Jubouri, H. A. Al-Jendeel, S. A. Rashid, and S. Al-Batty, "Green synthesis of porous carbon cross-linked Y zeolite nanocrystals material and its performance for adsorptive removal of a methyl violet dye from water," *Microporous and Mesoporous Materials*, vol. 356, no. April, p. 112587, 2023, https://doi.org/10.1016/j.micromeso.2023.112587

[24] M. S. Abdulrahman, A. A. Alsarayreh, S. K. A. Barno, M. A. Abd Elkawi, and A. S. Abbas, "Activated carbon from sugarcane as an efficient adsorbent for phenol from petroleum refinery wastewater: Equilibrium, kinetic, and thermodynamic study," *Open Engineering*, vol. 13, no. 1, 2023, https://doi.org/10.1515/eng-2022-0442

[25] T. Wang, M. Jiang, X. Yu, N. Niu, and L. Chen, "Application of lignin adsorbent in wastewater Treatment: A review," *Separation and Purification Technology*, vol. 302, p. 122116, 2022, https://doi.org/10.1016/j.seppur.2022.122116

[26] T. R. Sahoo and B. Prelot, *Adsorption processes for the removal of contaminants from wastewater: The perspective role of nanomaterials and nanotechnology*. Elsevier Inc., 2020. https://doi.org/10.1016/B978-0-12-818489-9.00007-4

ازالة البنزوثايوفين من محاكاة الوقود بواسطة الامتزاز وباستخدام المادة المازة $Ni/\ \gamma-Al_2O_3$: دراسة الاداء، الامتزاز والحركية

نوار حيدر يعقوب [١،*]، طارق محمد نايف [١]، زيد نضال شريف [٢]

١ قسم الهندسة الكيمياوية، كلية الهندسة، جامعة بغداد، بغداد، العراق
٢ جامعة كيرتن، قسم الهندسة الكيمياوية، استراليا

الخلاصة

تركز هذه الدراسة على ازالة الكبيرت الامتزازي للبنزوثايوفين من محاكاة الوقود باستخدام $Ni/\ \gamma-Al_2O_3$ كمادة مازة. فقد بحثت هذه الدراسة عن تأثير تحميل ايونات النيل ونسبتها على كفاءة الازالة.وقد تمايضا ايجاد افضل موديل حركي وايزوثرمي يتطابق مع العملية. وقد تم تشخيص المادة المعدلة بتقنيات عدة تشمل XRD, FESEM, EDS حيث كشفت هذه التقنيات عن نجاح عملية التحميل وبالنسب المطلوبة من ٢ الى ١٠ %. وقدم تم اجراء عملية ازالة الكبريت تحت ضروف مختلفة من كمية المادة المازة (0.2–1 g) وتركيز الكبريت الابتدائيppm 100–260 ونسبة تحميل النيكل(%2–10) و زمن التلامس (min 15–600). اظهرت النتائج نجاح عملية ازالة الكبريت العميق وبنسبة ازالة ٩٦% عند تركيز الكبريت الابتدائي ١٠٠ ولواجد غرام من المادة المازة عند درجة حرارة الغرفة والضغط الجوي علما ان نسبة تحميل النيكل كانت ١٠ % وبلغ زمن التلامس ٦٠٠ دقيقة بينما كانت اعلى سعة للامتزاز ٥٧,٢ ملغم/ غم عن ٢٦٠ جزء من الملون من الكبريت. وقد وجد ان الموديل الايزوثرمي لانماير هو الاكثر تطابقا مع عملية الازالة ٩٩,٩% وان الموديل الحركي سيدو الثاني هو الاكثر وصفا لهذه العملية ٩٩,٩%.

الكلمات الدالة: الومينا اوكساید، التبادل الايوني، ازالة الكبريت بالامتزاز، الايزوثرمية للامتزاز، الموديلات الحركية.